F. Schaefer, Ed., Plenum Press, New York, N.Y., 1977, p 1.
(13) R. H. Hughes, *J. Chem. Phys.*, **24**, 131 (1956).
(14) Y. Morino, Y. Kikuchi, S. Saito, and E. Hirota, *J. Mol. Spectrosc.*, **13**, 95 (1964).
(15) The previously noted[16,17] greater importance of central atom d functions in calculations on SO_2 compared to O_3 is, however, apparent.
(16) S. Rothenberg and H. F. Schaefer, *Mol. Phys.*, **21**, 317 (1971).
(17) S. Rothenberg and H. F. Schaefer, *J. Chem. Phys.*, **53**, 3014 (1970).
(18) If the energy lowerings produced by adding single d components are roughly additive, then the 28% contribution to the total SO_2 energy lowering produced by the d_{xy} orbital can at most be ~1.5 times the next largest contribution from a single d function, and this figure is only obtained in the unlikely event that the four non-symmetry-required components have equal energy lowering effects.
(19) H. Nakatsuji and J. I. Musher, *Chem. Phys. Lett.*, **24**, 77 (1974).
(20) Analogous results have been observed[21] in studies of ethylene episulfide, episulfoxide, and episulfone, although cases can be found in which the addition of d functions to similar sp bases does lead to changes in the ordering of the orbital energies. For example, for SF_6 calculations apparently comparable to those of section IIB lead to a change in the relative position of the $3e_g$ orbital energy.[22] Sulfur d functions are symmetry required to contribute to this orbital orbital pair. With a minimal basis much larger changes in the SF_6 orbital energies are observed on adding d functions[23] (compare, however, section III).
(21) M.-M. Rohmer and B. Roos, *J. Am. Chem. Soc.*, **97**, 2025 (1975).
(22) B. Roos, unpublished results quoted in ref 23.
(23) F. A. Gianturco, C. Guldotti, U. Lamanna, and R. Moccia, *Chem. Phys. Lett.*, **10**, 269 (1971).
(24) J. B. Collins, P. v. R. Schleyer, J. S. Binkley, and J. A. Pople, *J. Chem. Phys.*, **64**, 5142 (1976).
(25) I. H. Hillier and V. R. Saunders, *Chem. Commun.*, 1183 (1970).
(26) I. H. Hillier and V. R. Saunders, *Mol. Phys.*, **22**, 193 (1971).
(27) M. F. Guest, M. B. Hall, and I. H. Hillier, *J. Chem. Soc., Faraday Trans. 2*, **69**, 1829 (1973).
(28) P. J. Hay, *J. Am. Chem. Soc.*, **99**, 1003 (1977).
(29) All calculations were performed using the ATMOL3 suite of programs: V. R. Saunders and M. F. Guest, "ATMOL3 Users Guide", Science Research Council, Daresbury, Warrington, England.

A Simple Model of Bond Geometry and the Stereoactivity of Lone Pairs

H. Bradford Thompson,* Madeleine Wells, and Joan E. Weaver

Contribution from the Bowman-Oddy Laboratories, The University of Toledo, Toledo, Ohio 43606. *Received April 5, 1978*

Abstract: Bond angles and the stereoactivity of lone-pair electrons are predicted using a simple quantum mechanical model consisting of orbitals on a circle or ring, with Dirac δ functions representing bonds. Treatment of bonding in a plane is simple enough to be handled on a small minicomputer. The pattern of energetically favored bond angles shows the effect of stereoactive lone pairs and the expected changes with ligand electronegativity. The bond angle in water is predicted as 104.9° (experimental 104.5°). Predictions for other small molecules compare favorably with those from other simple treatments. The model intentionally omits Coulomb repulsions: the bond angle trends would appear to result from the Pauli exclusion principle.

I. Introduction

An understanding of the geometries of molecules and ions is basic to almost every field of chemistry. Accordingly, the configurations of covalent bonds around atoms have been studied extensively, and there are available today not only a vast body of experimental data, but also a number of well-documented and useful generalizations. Important among these is the effect of lone electron pairs upon the bond geometry about an atomic kernel. Concepts used to explain observed trends include hybridization,[1] valence-shell electron-pair repulsion (VSEPR),[2] second-order Jahn-Teller effects,[3] and ligand-pair vs. lone-pair electrostatic repulsions.[4] These schemes possess in common a recognition that bond geometries can generally be predicted from (1) the number of bond and lone pairs about each atom in a Lewis-type description and (2) the relative electronegativities of the atoms involved.

Two sources of the apparent stereoactivity of lone-pair electrons have been suggested: electrostatic repulsions and effects of the Pauli exculsion principle. Extreme partisans of each view can be cited.[5] In this paper we explore the simplest model we can imagine which might simulate the effect of the number of valence electrons on a bond angle. This model intentionally omits electrostatic repulsions. We believe that the success of this model in mimicking observed stereochemistry may be important in assessing the role of the Pauli principle, and in discussing bonding concepts in general.

A very preliminary report on this model has been published.[6] We here present it in detail, and dissect it in terms of localized orbitals, electron densities, and kinetic vs. potential energy contributions. We calculate bond angles for several simple molecules, and compare results with those from other models.

II. The Model and Its Exact Solutions

In this model the electrons are placed on a ring, that is, on the circumference of a circle, so that the position of each electron is defined by the value of a single angular coordinate, ϕ. This circle can be thought of as centered at the nucleus, and as having some radius appropriate for the purpose of examining angular electron-electron interactions, such as a typical bond radius. We are thus replacing orbital functions involving three coordinates by functions of only one angle: that in the plane of the bond. For a single electron the Schroedinger equation has the familiar solutions:

$$\psi_0^0 = 1/\sqrt{2\pi} \qquad W_0^0 = 0$$
$$\psi_{c,k}^0 = \cos(k\phi)/\sqrt{\pi} \qquad (1)$$
$$\psi_{s,k}^0 = \sin(k\phi)/\sqrt{\pi} \qquad W_k^0 = k^2 W_1^0$$

where k is an integer. The natural unit of energy in this model is W_1^0; all energies will be expressed in this unit, and this symbol will be omitted for the remainder of this paper. W_1^0 is approximately 6.104×10^{-39} J m$^2/r^2$, where r is the radius of our circle.

For this discussion we shall ignore Coulomb electron-electron repulsions. Equations 1 then give a set of orbitals to be doubly occupied by electrons. It was early pointed out by Lennard-Jones[7] that for three electrons of like spin occupying the three lowest orbitals on a circle or ring, the most probable electron-electron angular separation is 120°. Since the electrons of each spin move independently of those of opposite spin, it might be argued that if one electron of each spin (i.e., one pair) is pinned down at a given position by formation of a bond, electron density might pile up at positions 120° from that bond,

0002-7863/78/1500-7213$01.00/0

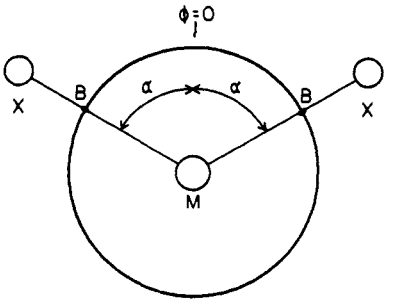

Figure 1. Triatomic molecule with the circle of this model superimposed. M and X are central and ligand nuclei. B is the point on the circle where the Dirac δ function representing the M–X bond is applied. This point is defined by the angle α from the reference direction $\phi = 0$. The bond angle is 2α.

thus creating the best location for a second bond. This is, of course, the known favored orientation of two bonds in the presence of three electron pairs in a plane, and is commonly described as sp^2 bonding.

The Model for One Bond. To test whether the restriction of one electron to a particular region of the ring does indeed create a buildup of charge at specific angles, a potential at the bond is required. Elaborate potentials could be devised to imitate the situation in specific molecules. However, the trends we hope to mimic are very general, so it seems appropriate to choose a very simple potential function. One such function is a Dirac δ function, $V = -\lambda\delta(\phi - \alpha)$. In such a function the potential is everywhere zero except at the angle $\phi = \alpha$, where there is a very narrow, deep potential well.[8] The quantity λ may be thought of as the product of the width and the depth of the well, and is in this model the analogue of the electronegativity of the atom at the other end of the bond. For the remainder of this paper the term "bond" will mean the location of such a potential function on the circle (see Figure 1). The use of the Dirac δ function leads to very simple exact solutions of the Schroedinger equation. Discussion of its appropriateness is reserved for a later section.

Everywhere except at a bond, the eigenfunctions will be sine and cosine functions similar to those in eq 1. At the bond the function will bend very sharply over an infinitesimal interval. This means that elsewhere this function can curve more gradually than a corresponding function in the absence of a bond, and still meet the closure conditions required on a circle. Thus curve c,1 in Figure 2 has curvature typical of a cosine curve of longer wavelength (and lower energy) than would be possible in the absence of the bond. For one bond located at 180°, the functions will be given by

$$\begin{aligned} \psi_0 &= N\cosh(a\phi) & W_0 &= -a^2 \\ \psi_{c,k} &= N\cos(ak\phi) & W_{c,k} &= a^2k^2 \\ \psi_{s,k} &= N\sin(ak\phi) & W_{s,k} &= a^2k^2 \end{aligned} \qquad (2)$$

where a is never greater than one except for $k = 0$. These equations define the functions on the interval $-\pi < \phi < \pi$. The constants a and N have unique values for each different orbital function ψ for each value of λ.

As is shown in detail in Appendix A, this leads to a very simple relationship between λ and the change in slope of the orbital at the bond:

$$(d\psi/d\phi)_+ - (d\psi/d\phi)_- = -\lambda\psi_b \qquad (3)$$

where ϕ_b is the value of ϕ at the bond, and the subscripts + and − refer to the slope just to the right and left, respectively, of the bond as shown in Figure 2. The appendix also shows in detail how a can be obtained. The wave functions of eq 2 with

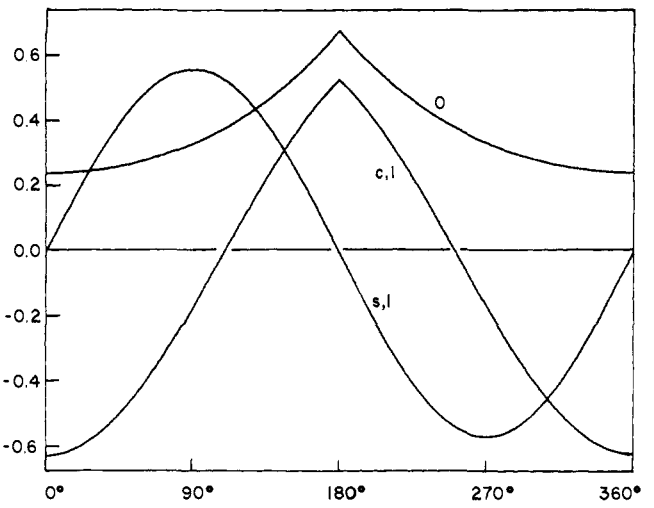

Figure 2. Canonical orbitals on a circle with one bond at 180°, λ = 1. The labels on the curves correspond to the subscripts in eq 2.

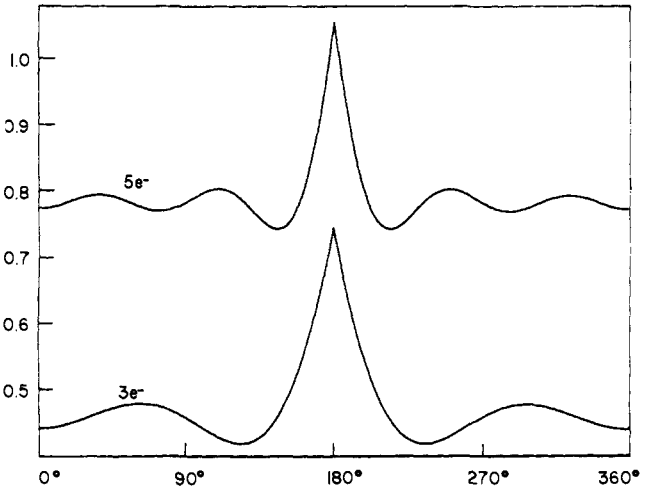

Figure 3. Electron densities for three and five electron pairs on a circle, λ = 1.

the proper a values inserted describe a complete orthogonal set of orbitals appropriate for occupancy by electrons.

Figure 2 shows the lowest three orbitals for λ = 1. As expected, the orbitals that do not have nodes at the bond now have cusps which lead to lowering of their energy. We can now proceed to examine the effects of the bond on the charge density distribution. The charge density at any point on the circle is given by

$$P(\phi) = \sum_{k'} n_{k'}\psi_{k'}^2 \qquad (4)$$

where $n_{k'}$ is the number of electrons in the orbital and the sum is over all the filled orbitals. The sets of subscripts in eq 1 and 2 (for instance, c, k) are here represented by a single index k'. For any odd number of electron pairs on a circle the charge density in the absence of a bond is uniform, since ψ_0^0 is constant, and for each k greater than zero $\sin^2(k\phi) + \cos^2(k\phi) = 1$. The two orbitals of the same k are the equivalent on the circle of a complete subshell. For three or five electron pairs with a bond present the charge density is shown in Figure 3. The density is far from constant, even in regions away from the bond. In addition to the peak at the bond, there clearly are secondary maxima spaced approximately evenly around the circle. In the three-electron case the maxima occur at 118° to either side of the bond for λ = 1, and 115° to either side for λ

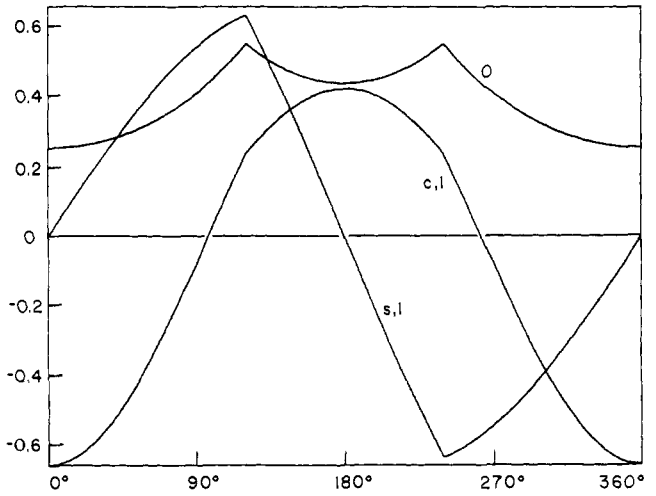

Figure 4. Canonical orbitals on a circle with bonds at 120 and 240°, λ = 1. Labels on the curves correspond to the subscripts in eq 5.

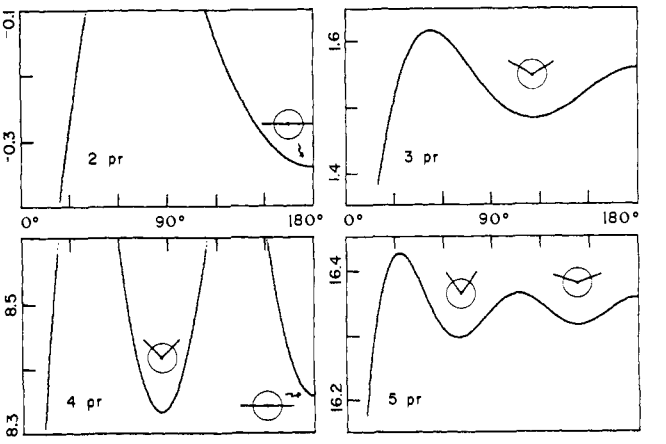

Figure 5. Energies for two bonds as a function of bond angle, for two, three, four, and five electron pairs. The small diagrams above the energy minima show the approximate bond angles.

Table I. Bond Angles for Minimum Energy

λ[a]	bond angle, deg			
	3 e⁻ pair	4 e⁻ pair[b]	5 e⁻ pair[c]	
0.5	117.9	88.1	70.6	143.5
1.0	115.4	86.1	69.2	143.0
1.5	112.3	83.9	67.7	142.5
2.0	108.7	81.6	66.1	142.0
2.5	104.9	79.2	64.4	141.4
0.0[d]	120	90	72	144

[a] Electronegativity variable; see text and eq 3. [b] For four-electron pair the minimum is for the s,2 orbital occupied. There is also a minimum at 180°, for the c,2 orbital occupied. [c] The energy minimum near 72° is in each case slightly deeper than that near 144°. [d] Extrapolated from the data above.

= 2. Thus these secondary maxima occur just where one would expect stereoactive lone pair electrons to be centered, and our speculation from Lennard-Jones' observations is fulfilled.

The Model for Two Bonds. From the above it clearly might be anticipated that two bonds in the presence of three electron pairs might be most stable if separated by about 120°, so that each bond could take advantage of the tendency of the other to produce a secondary maximum. This speculation can be tested directly. If two bonds are placed at $\phi = \alpha$ and $\phi = -\alpha$ as in Figure 1, the orbital functions are

$$\psi_0(\phi) = \begin{cases} N \cosh(a\phi) & 0 < \phi < \alpha \\ N' \cosh(a\{\pi - \phi\}) & \alpha < \phi < \pi \\ \psi_0(-\phi) & -\pi < \phi < 0 \end{cases}$$

$$\psi_{s,k}(\phi) = \begin{cases} N \sin(ak\phi) & 0 < \phi < \alpha \\ N' \sin(ak\{\pi - \phi\}) & \alpha < \phi < \pi \\ -\psi_{s,k}(-\phi) & -\pi < \phi < 0 \end{cases} \quad (5)$$

$$\psi_{c,k}(\phi) = \begin{cases} N \cos(ak\phi) & 0 < \phi < \alpha \\ N' \cos(ak\{\pi - \phi\}) & \alpha < \phi < \pi \\ \psi_{c,k}(-\phi) & -\pi < \phi < 0 \end{cases}$$

The energy is related to a just as in eq 2. Functions of this form for $k = 0$ and 1 are shown in Figure 4 for bonds at 120 and 240°. Both a and the ratio N/N' must be determined for each function. Equation 3 must apply at each bond, and furnishes one of the two conditions required. The other condition is that each wave function be continuous at the bond.

With two bonds, we have the opportunity to study the total energy as a function of bond angle. Since we have ignored electron-electron repulsions, the energy E is given by the sum of the occupied orbital energies. As previously reported,[6] the results display three effects in common with the VSEPR and other models: (1) bond angles clearly show the apparent stereoactivity of lone pairs; (2) bond pairs appear to take up less space than lone pairs; and (3) this "shrinkage" of the bond pairs appears to increase as the electronegativity of the ligands (as represented by λ) increases. Energy as a function of the bond angle (2α) is shown in Figure 5 for $\lambda = 1$. The optimum bond angles for various electronegativities and numbers of electron pairs are given in Table I. The bond angle extrapolated to $\lambda = 0$ is in each case $360°/n$ where n is the number of electron pairs. This is the result to be expected if bond-pair and lone-pair electrons are equally active sterically.

III. Localization

Transformation of sets of delocalized canonical orbitals to equivalent sets of localized orbitals has proved a powerful tool for dissecting molecular orbital descriptions into functions more closely corresponding to chemists' ideas of bonding and nonbonding electron pairs.[9] In general, the canonical orbitals are mixed by application of a unitary transformation such that some localization criterion is satisfied. For the one-bond, three-pair case above, localization turns out to be simple if we assume that there will be one bonding orbital η_1 peaking at 180° and two lone pair orbitals on either side, such that $\eta_2(\phi) = \eta_3(-\phi)$. We chose as our localization criterion minimum charge-density overlap from different orbitals.[10] Details are included in Appendix B.

Figure 6 shows the bond orbital, η_1, and its square or density function. This orbital clearly shows the cusp at 180°. The density plot for a nonbonding orbital, curve c in Figure 6, on the other hand, shows no cusp. Indeed, the function has a node very near the bond site. This suggests an alternate localization criterion: that the bond orbital be maximized and lone-pair orbitals minimized at the bond. This criterion is easily applied—details are included in Appendix B. The results from the two criteria are nearly identical.

Figure 7 shows the shape of the bond orbital as a function of λ. This orbital becomes sharper and more localized as λ increases. The nonbonding orbitals, on the other hand, show so little change with changing λ that on the scale of these figures the graphs are almost indistinguishable. The density maxima in the nonbonding orbitals are not at precisely 120°

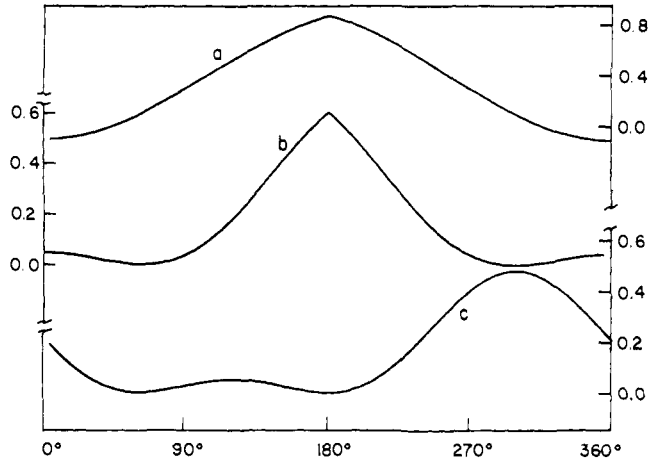

Figure 6. Localized orbitals on a circle with one bond at 180°, λ = 1, three electron pair: (a) the bond orbital η_1; (b) the bond-orbital electron density per electron η_1^2; (c) the electron density per electron in a lone-pair orbital η_2^2. The density in the other lone pair orbital, η_3^2, is obtained by reflecting curve c across the 180° line.

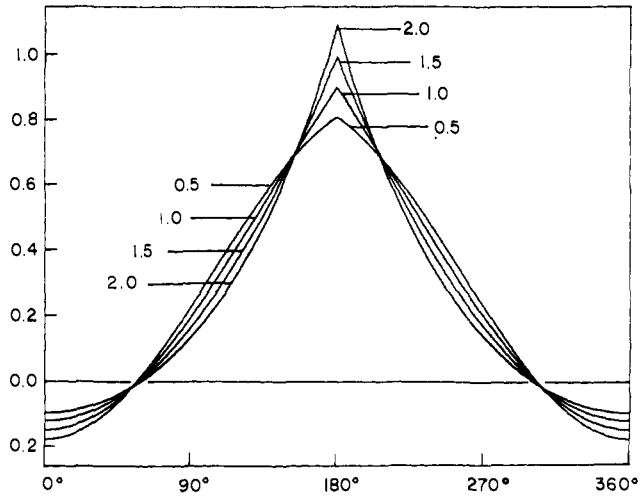

Figure 7. Localized bond orbital for varying λ. The labels on the curves are the respective λ values.

from the bond. For λ = 1, the maxima are at 61.5 and 198.5°; that is, 1.5° less than 120° from the bond. This is in the correct direction to account for the bond-angle shrinkage with increasing λ when two bonds are present, but is too small by a factor of 3 to account for the shrinkage (4.6°) shown in Table I.

The two-bond orbitals can be similarly localized, and the resulting two bond-pair orbitals and one lone-pair orbital resemble very closely those for the one-bond system. The lone-pair orbitals also closely resemble a localized orbital of sp^2 type with no bonds present. This suggests that lone-pair orbitals are little affected by the presence or strength of bonds, and that the causes of changes in bond angles and related properties are to be sought in changes in the bond orbitals. This might seem a trivial or obvious point, but explanations of the known geometries of SF_4 and ClF_3 have been given[2] which rely upon counting the number of 90° angles assigned to lone-pair–lone-pair interactions.

IV. Discussion

Appropriateness of the δ Potential. The Dirac δ function seems at first sight to be a violent approximation to the Coulomb effects which may make the bond region different from other regions around a central atom. However, it can easily be shown[8b] that in one dimension the δ function produces the sort of orbital expected (in three dimensions) for an electron in the neighborhood of a positive charge:

$$\psi(x) = N_x \exp(-z|x|) \tag{6}$$

where x is in units of Bohr radii and the positive charge is a fraction z of the electronic charge.

This is a replica in one dimension of a hydrogen-like 1s orbital. *The Dirac δ function is the one-dimensional surrogate of a point-charge Coulomb potential in three dimensions.* The change in slope at $x = 0$ is

$$(d\psi/dx)_+ - (d\psi/dx)_- = -2z\psi(0) \tag{7}$$

Suppose that the line along which x is measured corresponds roughly to a part of our circle. Then the above can be combined with eq 3 in order to estimate the effect of a charge on an orbital on a circle:

$$(d\psi/d\phi)_+ - (d\psi/d\phi)_- = -\lambda\psi = -2zr\psi \tag{8}$$

The factor r is the radius (in Bohr units) of our circle, and must be included owing to the shift from linear units (x) to angle (ϕ).

By using the δ function we are treating the bond as though it introduced a fractional charge at some specific radius, and the angular perturbation of the wave function at that radius was decisive in determining the bond angle. If we accept this interpretation, we must decide upon an appropriate combination of z and r. At small r, near the central nucleus, the orbitals are relatively far from the ligand nuclei, and their shapes are probably little affected by changes in angle. At large r, say near the bond distance, the molecular orbital functions will resemble a sum of contributions from the individual atomic orbitals, which will move independently with bond angle and show little of the type of interaction exhibited by the two cusps in Figure 4. Thus a radius r to which bond–bond effects might most typically apply would be an intermediate one, perhaps at a covalent radius. If we take r = 1.5 Bohr, then using λ = 1 implies that $z = 1/3$, and a bond region is taken to show the effect of about one-third of an electronic charge at the bond radius. Ligands with short bond radii and with high electronegativity would be expected to correspond to higher values of λ.

In most small molecules in which the stereoactivity of lone pairs is studied, a relatively electropositive central atom is surrounded by more electronegative ligand atoms.[11] Notable exceptions are hydrides, such as H_2S and PH_3. Bond angles in a species MH_n are usually at least as small as those in the analogous halides MX_n, in spite of hydrogen's lower electronegativity. In our model, hydrogens would be expected to mimic more electronegative ligands because the protons are deeply embedded in the charge cloud of the central atom. We use the δ function to represent either the localized effect of such a proton or the effect of a more remote, electronegative ligand: along a given circle that intersects the bond directions, these directions correspond to regions of low (more negative) potential energy. In these regions, in accord with the Schroedinger equation, orbital functions have a larger second derivative than they would exhibit in the absence of the ligand. This permits a smaller second derivative on the rest of the circle, which in turn implies a lowered value of the orbital energy. The antisymmetric function for two bonds $\psi_{s,l}$ (curve s,l in Figure 4) shows this effect very dramatically; curvature has been largely concentrated at the bond positions, and the energy of this orbital is only 0.376 W_1^0, about 3/8 of the energy of the corresponding orbital with no bonds present.

Application to the Bond Angle in Water. We can apply eq 8 to water as a simple test case. One of the nonbonding valence electron pairs in water occupies the p orbital perpendicular to the plane of our circle, and is outside the scope of our model. There are thus three valence electron pairs, two bonding and

Table II. Experimental and Calculated Bond Angles, AH_2 Molecules

species	bond length,[a] pm	bond angle, deg			
		exptl[a]	TSP[b]	this model[c]	this model[c] scaled
	Species with Six In-Plane Valence Electrons				
H_2O	95.72[d]	105	102	105	
H_2S	132.8	92	99	96	
H_2Se	146	91		93	
CH_2 $^1A_1$	111	102	100	101	
NH_2 $^2B_1$	102.4	103	101	103	
NH_2^-	103[d]	104[d]	100	103	
PH_2 $^2B_1$	142.8	92	99	94	
	Species with Five In-Plane Valence Electrons				
BH_2 $^2A_1$	118	131	118	113	130
AlH_2 $^2A_1$	159	119	117	109	118
CH_2 $^3B_1$	107.8[e]	136[e]	120	117	135
NH_2 $^2A_1$	100.4	144	120	119	138
PH_2 $^2A_1$	104.3	123	118	106	123

[a] Bond lengths and experimental angles, unless otherwise indicated, are taken from Herzberg (ref 13), Table 62. [b] The ion-lone-pair model of Takahata, Schnuelle, and Parr, ref 4. [c] Values of λ calculated from eq 8 using $z = 0.7$ as described for water. Scaled values were obtained using $z = 0.45$. [d] From Sutton, ref 12. [e] G. Herzberg and J. W. C. Johns, *J. Chem. Phys.*, **54**, 2276–2277 (1971).

one nonbonding, and these occupy the three orbitals for $k = 0$ and $k = 1$. Water is thus a filled-subshell case, as it should be since it possesses a simple Lewis structure.

The quantity z can be taken as a unit electron charge partially shielded by the presence of a second electron in the same orbital, assumed to behave near the bond like a 1s orbital. We will take $z = 0.7$ in accordance with Slater's rules. For r we will use the bond length, 1.8 Bohr or 96 pm.[12] This value is probably high: as noted above, the bond length is probably greater than the optimum radius for this model. However, the resulting λ value, 2.5, gives a minimum energy at a bond angle of 104.9°. Agreement with the experimental value[12] for water, 104.5°, must be considered fortuitously good; we do not claim this sort of precision for our model generally.

We can also predict a bending force constant for water. In terms of the energy unit W_1^0, energies at bond angles of 104, 105, and 106° are respectively 4.308 472 792, 4.308 550 296, and 4.308 420 425. Taking the second derivative of this energy from the second finite difference, this gives a bending force constant k_ϕ of 4.17×10^{-28} dyn cm^3/r^2, and we obtain 4.97×10^{-4} dyn cm^{-1} for k_ϕ/r^2, as compared with a commonly quoted experimental value of 7×10^{-4} dyn cm^{-1}.[13] This estimation depends critically upon the choice of the appropriate radius r, which enters the comparison taken to the fourth power. The agreement seems as good as should be expected. At least, comparative energies as here calculated correspond in magnitude to those in nature.

Application to Other AH_2-Type Molecules. The procedure used for water can be applied to other species with two bonds and three electron pairs on the ring. Results are given in Table II, and compared with those from a model by Takahata, Schnuelle, and Parr. The latter model depends on electrostatic repulsions alone to produce the bond angles. The two models are remarkably parallel in their input information. Each uses the experimental bond length, plus one screening constant obtained from Slater's rules. Each has no other adjustable parameters. Table I includes all AH_2 cases treated by Takahata et al. Clearly our model follows nature more closely than does the electrostatic model. Indeed, the electrostatic model does not represent at all well the observed difference between first-row and second-row hydrides, and has a very short range (99–102°) for all molecules of this type treated. Our model appears to underestimate this range also, but nowhere nearly so badly as the electrostatic treatment.

The case with five electrons on the ring can be treated by calculating energies with $\psi_{c,1}$ only singly occupied. Results are given in the lower half of Table II. Here neither model is very good, but again the electrostatic model predicts a very short range of angles, while our model imitates the experimental trends quite closely. This point can be emphasized by scaling our angles upward by adjustment of the factor z in eq 6–8. This leads to the remarkably good fit in the final column. A number of rationalizations for adjustment of z (or r) might be given. Clearly our model seems to fail in these open-shell cases in the direction indicating a smaller effect than expected of the bond potentials on the orbitals. One explanation that seems in accord with our arguments in developing our model is as follows. We have described the bond-directing effect in terms of the charge buildup created by each bond, and the secondary charge maxima which form favorable places for a second bond. With electrostatic repulsions ignored, the electrons of each spin set form a separate, independent problem. In the closed-shell case the electron densities for the two spins are identical. For the open-shell case with different numbers of electrons for different spins, however, the bond angle at which bonds can take maximum advantage of the density maxima for one spin is not the same as the optimum angle for the other spin. The angle of minimum energy will be a compromise in which *neither* bond can take best advantage of the effect of the other for electrons of *either* spin. Thus the changes of slope in eq 3 will be less than in the closed-shell case, because on the average the values of ψ_b will be lower. We can apparently simulate this effect by a scalar reduction in λ.

That we can "predict" bond angles well in six-electron cases, and reproduce bond angle trends even in open-shell five-electron cases, is evidence that bond geometry can be described by a model that does not employ specific electrostatic bond-directing forces.

AH_2 Orbital Energies. Figure 8 shows the effect on orbital energies of addition of the first and the second bond, and upon the two-bond energy as the bond angle is changed. The results can be compared with those discussed by Walsh.[14a] With no bonds present, there is a single lowest orbital on the circle, and then an energy-degenerate pair for each value of k. Upon addition of the first bond each pair is split, since the sine-type orbital has a node at the bond, and its energy is unaffected. With two bonds present, both orbitals are affected by bonds, and the energies are angle dependent as shown at the right of Figure 8. The lowest three orbitals have the same general angle dependence as given by Walsh, except for two details. We show

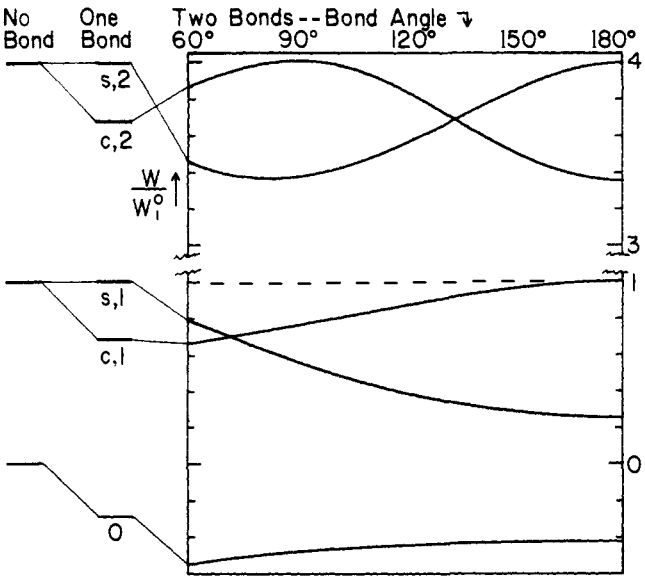

Figure 8. Orbital energies as a function of bond placement. $\lambda = 1$.

the energy crossover between the second and third lowest orbitals at about 70°, while Walsh shows it to be above 90°; and our lowest orbital is slightly lower in energy at low angles than at high angles, while Walsh predicted the reverse. Walsh's diagram for AH_2 molecules included an orbital (antisymmetric to the molecular plane) which is unaffected by changing bond angle. This perpendicular p orbital is, of course, not treated in our model, but its energy must be that of an unperturbed orbital with $k = 1$. This orbital is indicated by the dotted line, to facilitate comparison with Walsh's diagram.[14b]

The two orbitals shown for $k = 2$ are not treated by Walsh for the AH_2 case, and are not occupied for any of the AH_2-type molecules in the preceding section. However, their energies will contribute to the four-pair and five-pair cases.

Kinetic vs. Potential Energy Effects. It might on first examination appear that since the energy of an orbital on a circle is calculated from its second derivative (via the quantity a^2), the energy changes caused by bonds are kinetic energy effects, and that a lowered orbital energy means a lowered orbital kinetic energy. This would run counter to the virial theorem, under which a lowered total energy corresponds to a lowered potential energy but to an increased kinetic energy. The above view of our model would be incorrect because it ignores the contributions to both potential and kinetic energies due to the bond. The total energy $W_{k'}$ is a constant of motion for the electron, and since there is no potential energy except at the bond, $W_{k'}$ equals the kinetic energy elsewhere. At the bond there is a potential energy, which by the definition of the δ function integrates to $-\lambda\psi_b^2$. There is also a kinetic energy component at the bond, corresponding to the sharp bend in the wave function, $\lambda\psi_b^2$, of the same magnitude as the potential energy but positive in sign. For the wave function ψ_0 for one bond and $\lambda = 1$, the energy is $-0.287\ 03$, which is also the kinetic energy contribution for the region not at the bond. At the bond, $\lambda\psi_b^2$ is $0.465\ 70$, so the potential energy is $-0.465\ 70$ and the total kinetic energy is $0.178\ 67$. Since for this orbital, both kinetic and potential energy are zero in the absence of a bond, the bond potential has caused the *total* kinetic energy to rise, although the contribution from the region not at the bond has decreased. The same trends are discovered upon analysis of other orbitals studied.

"Pauli Forces" and the Source of Bond Directing Effects. Extensive discussion as to the underlying reasons for bond-direction trends has centered about the relative importance of Coulomb repulsions on the one hand and effects due to the Pauli exclusion principle on the other.[5] The latter have been called "Pauli forces" by some. This seems to us an unfortunate terminology, unless one can define a "Pauli density".

In the present work explicit electron-electron repulsions were intentionally omitted, but the exclusion principle was not. To the degree that our simple system mimics nature, we then have a strong indication that the exclusion principle plays a major role in producing the trends mimicked. However, to claim that we have shown, even within this model, that the exclusion principle produces these trends independent of Coulomb contributions would be an overstatement, since Coulomb effects enter our model in at least three ways. (1) The electrons are held in the vicinity of a central nucleus by nuclear-electron attractions, and are viewed as being at some particular radius, determined partly by nuclear screening effects; that is, by generalized repulsions of electrons for each other. (2) Although each curve in Figure 5 shows a deep minimum in energy at a bond angle of zero, this angle is not taken as realistic, since nuclear mutual repulsions (which have also been ignored) make it prohibitive. (3) The region of each bond is supposed to differ from other regions of the circle by virtue of a lower potential energy, due to only partially screened nuclear attraction of the ligand nucleus.

Thus in our model Coulomb and Pauli effects are so intimately entwined that separate evaluation is not possible. We respectfully suggest that our treatment is perhaps not unique in this respect. However, none of the Coulomb contributions of the preceding paragraph can, individually or in combination, produce energy minima such as those in Figure 5. At least within this model, the Pauli exclusion principle seems dominant in determination of stable geometries.

Acknowledgments. We are grateful to Professor L. S. Bartell for discussions which stimulated this work and for his continued interest and encouragement, and to Professor E. Jean Jacob for her thoroughgoing criticism of both the substance and the details of this paper. We also gratefully acknowledge a Faculty Research Award from the University of Toledo, which supported and sustained us during the summer when most of this work was done.

Supplementary Material Available: Appendix A (solution of the Schroedinger equation) and B (localization), with four tables (6 pages). Ordering information is given on any current masthead page.

References and Notes

(1) See L. Pauling, "Nature of the Chemical Bond", Cornell University Press, Ithaca, N.Y., 1939, Chapter III, and references cited therein.
(2) R. J. Gillespie and R. S. Nyholm, *Q. Rev., Chem. Soc.*, **11**, 339–380 (1957); R. J. Gillespie, *J. Am. Chem. Soc.*, **82**, 5978–5983 (1960); "Molecular Geometry", Van Nostrand-Reinhold, Princeton, N.J., 1972.
(3) L. S. Bartell, *J. Chem. Educ.*, **45**, 754–767 (1968); R. G. Pearson, *J. Am. Chem. Soc.*, **91**, 1252–1254, 4947–4955 (1969).
(4) (a) Y. Takahata, G. W. Schnuelle, and R. G. Parr, *J. Am. Chem. Soc.*, **93**, 784–785 (1971); (b) G. W. Schnuelle and R. G. Parr, *ibid.*, **94**, 8974–8983 (1972); (c) R. G. Parr and G. W. Schnuelle in "Conformation of Biological Molecules and Polymers. The Jerusalem Symposia on Quantum Chemistry and Biochemistry, V", The Israel Academy of Sciences and Humanities, Jerusalem, 1973, pp 737–745; (d) see also A. W. Searcy, *J. Chem. Phys.*, **28**, 1237–1242 (1958).
(5) Approaches depending strongly on the exclusion principle include, in addition to that of Gillespie et al. (ref 2), that of H. A. Bent, *J. Chem. Educ.*, **40**, 446–452, 524–530 (1963), and of J. W. Linnett, *J. Am. Chem. Soc.*, **83**, 2643–2653 (1961); "The Electronic Structure of Molecules", Methuen, London, 1964. A recent rebuttal to the "Pauli force" concept is that of J. L. Bills and R. L. Snow, *J. Am. Chem. Soc.*, **97**, 6340–6342 (1975).
(6) H. B. Thompson, *J. Am. Chem. Soc.*, **97**, 5293–5294 (1975).
(7) J. Lennard-Jones, *Adv. Sci.*, **11**, 142 (1954).
(8) (a) The treatment of a Dirac δ function implied here is not that preferred by mathematicians, but it will suffice for this application, and will give intuitive meaning to the quantity λ. (b) A good discussion of the δ function and its application to one-dimensional orbitals is given in F. C. Goodrich, "A Primer of Quantum Chemistry", Wiley-Interscience, New York, N.Y., 1972, Chapter 10.
(9) C. A. Coulson, *Trans. Faraday Soc.*, **38**, 433–444 (1942); J. Lennard-Jones, *Proc. R. Soc. London, Ser. A*, **198**, 1–13 (1949); C. Edmiston and K. Ruedenberg, *Rev. Mod. Phys.*, **35**, 457–465 (1963); W. England, L. S.

Salmon, and K. Ruedenberg, *Fortschr. Chem. Forsch.*, **23**, 31–123 (1971). See also R. B. Davidson, *J. Chem. Educ.*, **54**, 531 (1977), and references cited therein.
(10) W. von Niessen, *J. Chem. Phys.*, **56**, 4290–4297 (1972).
(11) See ref 4b, p 8977, and ref 4c, p 738.
(12) Averaged experimental values for water are taken as follows: O–H distance, 0.9572 Å (95.72 pm); bond angle, 104.52°. See "Tables of Interatomic Distances and Configuration in Molecules and Ions. Supplement", *Chem. Soc., Spec. Publ.*, **No. 18**, M37s (1965).
(13) G. Herzberg, "Molecular Spectra and Molecular Structure. II. Infrared and Raman Spectra of Polyatomic Molecules", Van Nostrand, Princeton, N.J., 1945, pp 170 and 187.
(14) (a) A. D. Walsh, *J. Chem. Soc.*, 2260–2266 (1953); (b) *ibid.*, 2262 (1953).

Free Energy Correlation of Rate Constants for Electron Transfer Quenching of Excited Transition Metal Complexes

R. Ballardini,[1a] G. Varani,[1a] M. T. Indelli,[1a] F. Scandola,*[1a] and V. Balzani*[1b]

Contribution from Centro di Studio sulla Fotochimica e Reattività degli Stati Eccitati dei Composti di Coordinazione del C.N.R., University of Ferrara, Ferrara, Italy, and Istituto Chimico "G. Ciamician", University of Bologna, Bologna, Italy.
Received November 18, 1977

Abstract: The quenching of the emitting excited states of $Cr(bpy)_3^{3+}$, $Ru(bpy)_3^{2+}$, and $Ir(Me_2phen)_2Cl_2^+$ (bpy, 2,2′-bipyridine; Me_2phen, 5,6-dimethyl-1,10-phenanthroline) by some 30 amines or methoxybenzenes having variable oxidation potentials has been studied in acetonitrile solution. Flash photolysis experiments showed that the quenching process takes place with formation of the one-electron oxidation product of the quencher. The bimolecular quenching constants obtained from the Stern–Volmer constants and the excited-state lifetimes have been found to be related to the free-energy change of the electron transfer process. The plots of log k_q vs. $E_{1/2}(Q/Q^+)$ show a region of linear increase at high $E_{1/2}$ values and reach a plateau at low $E_{1/2}$. With aromatic amines and methoxybenzenes as quenchers, the comparison between theoretical curves[14,16] and experimental plots indicates that the kinetically estimated value of the excited-state reduction potential is in reasonable agreement with that expected on spectroscopic grounds. The results also indicate that the intrinsic barrier for the excited-state self-exchange reaction is comparable with that of the ground-state self-exchange reaction. For $Cr(bpy)_3^{3+}$ and $Ir(Me_2phen)_2Cl_2^+$, no evidence of k_q decrease with $-\Delta G$ is present even for free-energy changes which are two to three times larger than that expected for the onset of the Marcus "inverted" region. The difference between the electron transfer quenching properties of aromatic and aliphatic amines is also briefly discussed.

Introduction

Electronic excitation decreases the ionization potential and increases the electronic affinity of a molecule.[2] As a consequence, those electronically excited states which live long enough to encounter other species can easily be involved in intermolecular electron transfer reactions. The extraordinary redox properties of electronically excited molecules are currently drawing the attention of many workers for at least two reasons: (1) they can be used for the conversion of light energy (including solar energy) into chemical energy[3-5] and (2) they allow us to check the theories of outer-sphere electron transfer reactions[6,7] over a broad range of free-energy change.[8-11]

The electron transfer reactions of electronically excited organic molecules have been extensively studied in the past decade,[12-37] particularly by Weller et al.[12-19] A quantitative analysis was given by Rehm and Weller,[14,16] who established an equation on the relationship between the rate constant and the free-energy change of the electron transfer process. Such an equation was found to be obeyed by a number of systems consisting of fluorescent aromatic hydrocarbons and various quenchers (amines, methoxybenzenes, nitriles). In the last few years it has been shown that transition metal complexes containing bpy (2,2′-bipyridine) or phen (1,10-phenanthroline) as ligands are very suitable for excited-state electron transfer reactions. Several theoretical and practical aspects (including solar energy conversion[3,4]) of these reactions have been studied[3-5,38-56] but with few exceptions[41,51,52] the correlation between rate constants and free-energy change has not yet been investigated.

We report here the results of a systematic study on the electron transfer quenching of excited $Cr(bpy)_3^{3+}$, $Ru(bpy)_3^{2+}$, and $Ir(Me_2phen)_2Cl_2^+$ by some 30 quenchers having variable oxidation potentials.

Experimental Section

Materials. Tris(2,2′-bipyridine)chromium(III) perchlorate hemihydrate, $[Cr(bpy)_3](ClO_4)_3 \cdot \frac{1}{2}H_2O$, was prepared and purified according to the procedure indicated by Baker and Mehta.[57] Tris(2,2′-bipyridine)ruthenium(II) chloride tetrahydrate, $[Ru(bpy)_3]Cl_2 \cdot 4H_2O$, was prepared and purified as indicated by Burstall.[58] A pure sample of *cis*-dichlorobis(5,6-dimethyl-1,10-phenanthroline)iridium(III) chloride trihydrate, $[Ir(Me_2phen)_2Cl_2]Cl \cdot 3H_2O$, was obtained as previously reported.[59] The quenchers were of the highest purity commercially available and were used without further purification. Tetraethylammonium perchlorate (TEAP) was C. Erba RS grade for polarography and was dried before use. Acetonitrile (Merck Uvasol) was used without further purification.

Apparatus. The emission spectra were measured with a Perkin-Elmer MPF 3 spectrofluorimeter equipped with an R-446 Hamamatsu tube for the experiments with the chromium complex and an R-106 Hamamatsu tube for those with the ruthenium and iridium complexes. The excitation wavelengths were 350 nm for $Cr(bpy)_3^{3+}$, 450 nm for $Ru(bpy)_3^{2+}$, and 400 nm for $Ir(Me_2phen)_2Cl_2^+$; the monitoring wavelengths were those corresponding to the maxima of the respective emission bands ($Cr(bpy)_3^{3+}$, 727 nm; $Ru(bpy)_3^{2+}$, 610 nm; $Ir(Me_2phen)_2Cl_2^+$, 495 nm). The lifetime of the emitting state of $Cr(bpy)_3^{3+}$ was obtained by measuring the decay of the doublet–doublet absorption (λ_{max} 390 nm) with an Applied Photophysics ruby laser apparatus. The emission lifetimes of the ruthenium and iridium complexes were measured by means of a modified Applied Photophysics apparatus based on the single photon counting technique. The excitation wavelength was 337 nm. The emission decay was monitored at the maxima of the respective emission bands. Transient absorption spectra were obtained by using an Applied Photophysics KR-10 flash photolysis apparatus.

0002-7863/78/1500-7219$01.00/0